ORIGINAL ARTICLE

Singularity theories and methods for characterizing mineralization processes and mapping geo-anomalies for mineral deposit prediction

Qiuming Cheng [a,b,c,*], Pengda Zhao [a,b]

[a] *State Key Laboratory of Geological Processes and Mineral Resources, China University of Geosciences, Wuhan 130087, China*
[b] *State Key Laboratory of Geological Processes and Mineral Resources, China University of Geosciences, Beijing 100083, China*
[c] *Department of Earth and Space Science and Engineering, Department of Geography, York University, Toronto M3J1P3, Canada*

Abstract In this paper, we show that geo-anomalies can be delineated for mineral deposit prediction according to singularity theories developed to characterize nonlinear mineralization processes. Associating singularity and geo-anomalies makes it possible to quantitatively study geo-anomalies with modern nonlinear theories and methods. This paper introduces a newly developed singularity analysis of nonlinear mineralization processes and nonlinear methods for characterizing and mapping geo-anomalies for mineral deposit prediction. Mineral deposits, as the products of singular mineralization processes caused by geo-anomalies, can be characterized by means of fractal or multifractal models. It has been shown that singularity can characterize the degree of geo-abnormality, and this has been demonstrated to be useful for mapping anomalies of undiscovered mineral deposits. The study of mineralization and mineral deposits from a nonlinear process point of view is a new but promising research direction. This study emphasizes the relationships between geo-anomalies and singularity, including singular processes resulting in singularity and geo-anomalies, the characterization of singularity and geo-anomalies and the identification of geo-anomalies for mineral deposit prediction. The concepts and methods are demonstrated using a case study of Sn mineral deposit prediction in the Gejiu mineral district in Yunnan, China.
© 2011, China University of Geosciences (Beijing) and Peking University. Production and hosting by Elsevier B.V. All rights reserved.

* Corresponding author. Department of Earth and Space Science and Engineering, Department of Geography, York University, Toronto M3J1P3, Canada.
*E-mail address:* qiuming@yorku.ca (Q. Cheng).

1. Introduction

Delineating geo-anomalies to assist in finding mineral deposits has been a common practice in the fields of mineral exploration and mineral resource assessment. Studies on the relationship between geo-anomalies and occurrences of mineral deposits conducted by Zhao and his group in China since the late 1980s have led to new ideas and approaches for mineral deposit studies and for mineral resource quantitative assessments (Zhao and Chi, 1991; Zhao, 2002, 2007; Zhao et al., 2005). For example, the concepts of
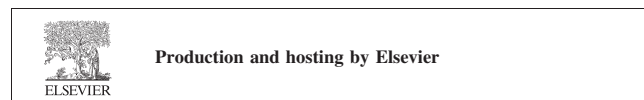
geo-anomalies and methods have been successfully applied in China for various types of mineral deposit predictions. Unlike the anomaly concept applicable to exploration geochemistry and geophysics, a geo-anomaly is referred to in Zhao (2002) as an area with significant geological differences from its surroundings in terms of factors such as composition, texture, structure and genesis. Whereas anomalies defined in geochemistry and geophysics can be delineated quantitatively with thresholds, some geological anomalies may not be easily quantitatively defined due to their complexity. Nevertheless, due to the differences between geological anomalies and surrounding areas, anomalies can often be identified through comprehensive geological, geochemical and geophysical surveying and mapping. Thus, geo-anomaly recognition methods can be employed in delineating target areas for mineral exploration.

In addition to mapping geo-anomalies for mineral deposit prediction purposes, studies of geo-anomalies are also beneficial for characterizing the fundamental properties of mineralization processes and mineral deposits. How do geo-anomalies occur? What are the fundamental properties of geo-anomalies? What can the dynamics of mineralization resulting in geo-anomalies? How are the formation and spatial-frequency-temporal properties of geo-anomalies be simulated? How are geo-anomalies mapped for mineral deposit prediction? Answers to these questions are essential not only for understanding the dynamics of mineralization and quantifying the spatial-frequency-temporal distributions of mineral deposits, but also for identifying geo-anomalies for mineral deposit prediction.

Recent studies have demonstrated that various types of hazardous geo-processes, such as earthquakes, volcanoes, floods, cloud formation, rainfall, hurricanes, landslides and mineralization processes, often result in anomalous amounts of energy release or mass accumulation that are generally confined to narrow intervals in time or space (Cheng, 2007a). The above property of anomalous amounts of energy release or mass accumulation is termed a singularity, and these types of processes are considered as singular processes (Cheng, 1999, 2007a). Singularity is a generic property of nonlinear natural processes that often generate end products depicting fractality or multifractality (Cheng, 2007b, 2007c; Cheng

and Agterberg, 2009). Hydrothermal processes in the Earth's crust can result in ore deposits characterized by high concentrations of metals with fractal or multifractal properties (Mandelbrot, 1989; Agterberg, 1995; Cheng, 2007d). The total amounts of ore and metals in hydrothermal ore deposits often have Pareto tails (Turcotte, 1997). Pareto distribution can be considered as an extreme value distribution, which is an important subject in mathematical geosciences. An invited paper meeting (IPM) on "extreme value statistics" was organized by the International Association for Mathematical Geosciences (IAMG) during the 53rd International Statistics Institute (53rd ISI). Two invited papers were presented at the conference: one covers the concept and methods of geo-anomalies with application in China (Zhao and Chen, 2001), and the other introduces singularity and multifractal filtering techniques to decompose anomalies from the background for mineral deposit prediction (Cheng, 2001). A fundamental property of singular processes is that their end products often show geo-abnormalities in some aspects. The rest of this paper will discuss a case study of Sn mineral deposit prediction and will demonstrate applications of nonlinear methods for the quantitative delineation of geo-anomalies for mineral potential prediction.

2. Materials and data

The study area chosen was the Gejiu mineral district located in southern Yunnan, approximately 200 km south of the city of Kunming, the capital of Yunnan Province (Fig. 1). This area is known for its world-class Sn mineral deposits and Sn production. Geological units within the main study area consist primarily of a sequence of Paleozoic−Mesozoic sedimentary (Gejiu Formation and other formations) and igneous rocks. Proterozoic low-grade metamorphic sand-shale rocks are mainly distributed in the southern part of the study area (Zhuang et al., 1996).

Two main types of igneous rocks were mapped: Paleozoic volcanic rocks and Mesozoic intrusive rocks. The former are mainly basalts, including the widespread Ailaoshan basalts within the extended study area (Zhuang et al., 1996). The intrusive Mesozoic
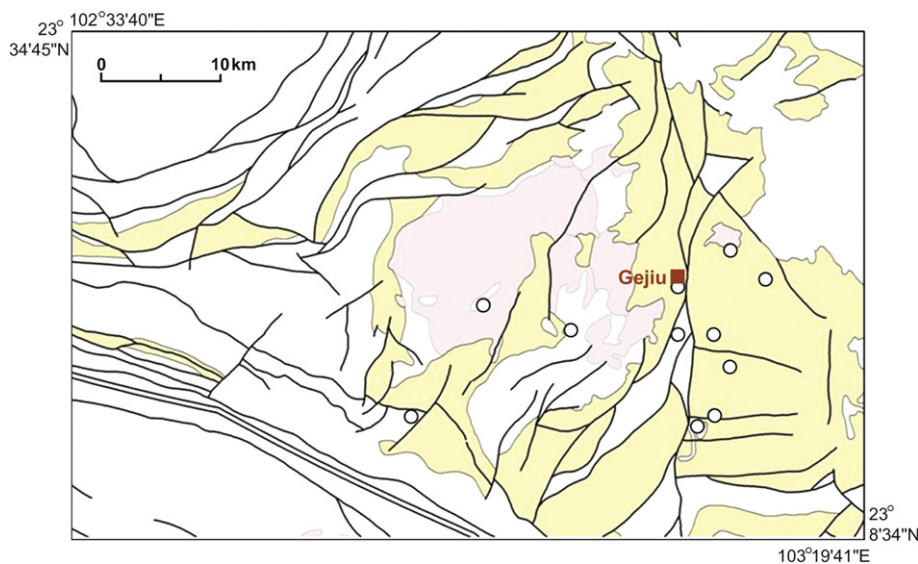

Figure 1 Simplified geology of the Gejiu mineral district. Pink polygons distributed in the center of the study area indicate felsic intrusions of the Gejiu batholith; yellow polygons indicate limestone of the Gejiu Formation; black lines represent faults, white areas represent other sedimentary rocks, and dots indicate Sn mineral deposits.

rocks are predominantly biotitic granitoid rocks including granite, monzogranite and plagiogranite. Mafic and ultramafic intrusive rocks are scattered throughout the study area. The Gejiu batholith is a complex granitoid complex located in the center of the study area with an outcrop area of about 450 km^2. This intrusion has been considered as one of the main controlling factors for Sn mineralization because several large Sn mineral deposits are found near the batholith. The main ore bodies formed in the Gejiu Formation, which is dominated by limestone with minor dolomites.

The area has gone through a long history of tectonic and complex structural activity, resulting in fault and fold systems at various scales and in various orientations, as shown on the map (Fig. 1). Fault systems control the general configuration of the mineralization and distribution of ore bodies. The main trend of mineralization in the central area is NNE−SSW, but the ore fields are concentrated along the intersections of NNE−SSW and E−W faults.

It has been generally accepted that Sn and Cu mineralization are associated with Gejiu Formation sedimentary country rocks and igneous bodies, particularly the Gejiu batholith, which were intruded into folded limestone deposited during the Middle Triassic. The enrichment of Sn, Cu and other metals occurred in and near the contact zone between the granite and wall rock through metamorphic, contact-metasomatic, and vein-filling processes. Ore types found in the contact and wall rock zones surrounding the batholiths include skarn, interlayered ores in the wall rocks, vein-type ores in fractures, and placer ores on the paleosurface.

The study area is covered by about 3800 evenly distributed stream sediment samples at a 2 km × 2 km (4 km^2) spatial resolution. Samples were collected and analyzed with a density of one mixed sample per 4 km^2 area by the Chinese National Geochemical Mapping Project as part of the Regional Geochemistry National Reconnaissance (RGNR) Project initiated in 1979 (Xie et al., 1997). For each sample, the concentrations of 39 geochemical elements and seven oxides were measured. For demonstration purposes, the data used in this paper are geochemical concentration values of six trace elements (Sn, Cu, Pb, Zn, As and Cd). Further details on the sampling and analysis of the stream sediment data can be found in Xie et al. (1997). The trace elements and their associations with Sn mineralization in the area were previously studied for mineral deposit predictions and for environmental assessments (Cheng, 2007a; Cheng and Agterberg, 2009; Cheng et al., 2009). The main objective of the reuse of these data in the current study is to demonstrate various new nonlinear concepts and models applicable to the characterization of mineralization and the mapping of geo-anomalies for mineral deposit prediction.

3. Fundamental characteristics of nonlinear geo-processes: singularity and geo-anomaly

3.1. Nonlinearity and power-law distribution

There are many types of nonlinear geo-processes that can cause end products with nonlinear properties when changing temporal or spatial scales. Geophysical and geochemical fields are used for mapping and exploration purposes. The change rates of these geophysical and geochemical quantities with changes of support may provide information characterizing the nonlinear property of geo-processes. For example, if a quantity ($Q(t)$) involved in a dynamic system changes through time (t), then the change rate of the quantity can be expressed as the first-order derivative $\frac{dQ(t)}{dt}$ if the first-order derivative exists. For a simple linear system, the change rate $\frac{dQ(t)}{dt}$ is related to the quantity $Q(t)$ with a constant decay rate τ (a value >0), for example,

$$\frac{dQ(t)}{dt} = -\tau Q(t) \tag{1}$$

This equation indicates that the change rate of the quantity in a dynamic system is proportional to the magnitude of Q with a negative constant decay rate τ. The solution of Eq. (1) can be expressed as $Q(t) = ce^{-\tau t}$. This exponential function has the excellent smooth property of having finite derivatives of any orders. The high-order derivatives of $Q(t)$ remain the same original function $Q(t)$ except for a constant; for example, the nth-order derivative is $\tau^n Q(t)$. The dynamics governed by Eq. (1) usually represent a system in a constant and uniform media so that the change rate is exponentially related to the time. There are many such systems in the geosciences, for example, rivers flowing in simple drainage networks due to the gravity potential differences of water heads and isotope decay rates in rock samples (which is used for geological dating). However, if the media in which a system is involved is heterogeneous for example, if a system involves a decreasing change rate through time according to the following equation,

$$\frac{dQ(t)}{dt} = -\frac{\tau}{t} Q(t) \tag{2}$$

where the change rate is proportional to $Q(t)$ with a variable decay rate $-\tau/t$ that decreases with increasing time, then, as time goes on, the decay rate of the system becomes more rapid. The solution of the system as expressed in Eq. (2) is a power-law function: $Q(t) = ct^{-\tau}$. According to this function, the system approaches infinity when the time is close to zero. As opposed to the exponential function, the power-law function does not have a smooth property when $t \to 0$. In fact, the function does not have any positive-order finite derivatives when $t \to 0$, as shown below:

$$\frac{d^n Q(t)}{d^n t} = (-1)^n \frac{\tau(1+\tau)\cdots(n+\tau)}{t^n} Q(t) \tag{3}$$

The power-law solution of System (2) becomes singular when the time is too close to zero and when the actual system does not converge at the point where $t = 0$. As the system is usually a stochastic system so that Eqs. (1) to (3) are statistically held to be true, the actual system becomes chaotic or disordered (for example, with random walking processes) when close to singularity. This implies that not only the quantity but also the variances of the quantity of the anomalies or disordered region must be anomalously different from those in the background and ordered region.

The above discussion is based on simple dynamic systems with the temporal attribute t; similarly, we can discuss the spatial aspects of a system with a spatial attribute. If we consider mineralization as a nonlinear process and the anomalous element concentration in rocks or other types of media as the result of mineralization, denoting the concentration density value in small set A (an area for a 2D problem), then the change rate of the concentration due to a change of scale can be expressed as two forms:

$$\frac{d\langle \rho(A) \rangle}{dA} = -\tau \langle \rho(A) \rangle, \rho(A_0) = \rho_0 \tag{4}$$

$$\frac{d\langle \rho(A)\rangle}{dA} = -\frac{\tau}{A}\langle \rho(A)\rangle, \rho(A_0) = \rho_0 \tag{5}$$

where A is an areal set in a 2D space (spatial scale), $\rho(A)$ is the density of elements defined in set A, and τ is the decay rate of the dynamic system. Eqs. (4) and (5) can also be represented as 3D forms if the 2D set A is replaced by a volume set. For convenience, without a loss of generality, only the 2D system will be considered as an example in the following discussions.

The solutions of the two systems governed by Eqs. (4) and (5) can be obtained as follows:

$$\rho(A) = \rho(A_0)e^{-\tau(A_0 - A)} \tag{6}$$

$$\rho(A) = \rho(A_0)\left(\frac{A}{A_0}\right)^{-\tau} \tag{7}$$

The exponential solution (6) from System (4) and the power-law solution (7) from (5) show different properties, especially for a very small area A. To demonstrate the relationships between the models in (6) and (7), the concentration values of element As (ppm) in stream sediment samples collected from the Gejiu district are plotted as a map with a 2-km spatial resolution (seen in Fig. 2). The patterns in Fig. 2 show that high values of As are generally distributed in the eastern study area where several large Sn mineral deposits are found. We chose one location labeled as a green circle on the map in Fig. 2 to examine how the concentration density value calculated within square windows changes with window size. Fig. 3 illustrates the distribution of concentration density values calculated with square windows of sizes ranging from 2, 6 and 10 km to 26 km. The vertical axis represents the values of concentration density (ppm/km^2), and the horizontal axis indicates the linear size of the windows (km). Dots represent the actual data, solid lines are fitted by a least square method with a power-law model, and dashed lines are fitted with an exponential model. The results obtained from the least square fitting are estimated as $\rho(A) = 332.43\epsilon^{-0.416}$ with correlation coefficient $R^2 = 0.98$ and $\rho(A) = 212.77e^{-0.039\epsilon}$ with $R^2 = 0.801$. The
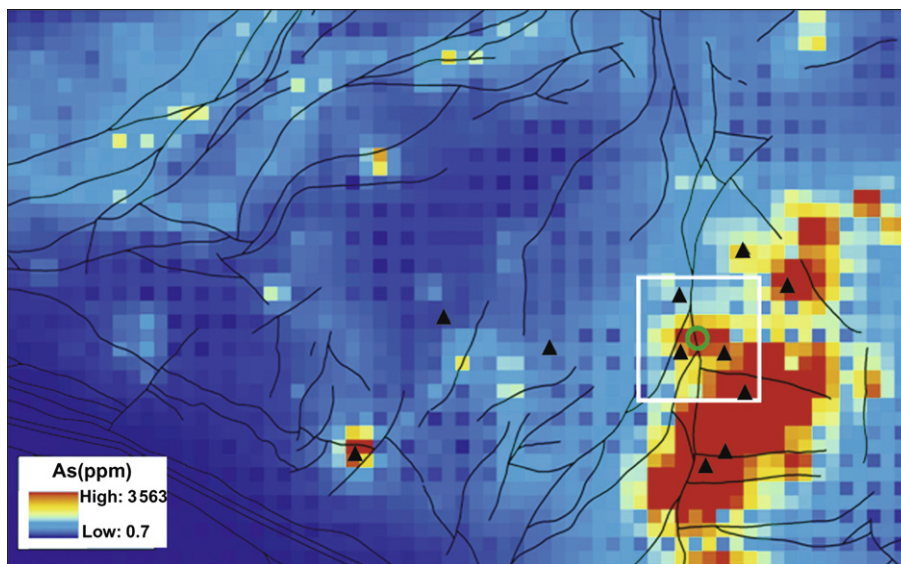
Figure 3 Relationship between the exponential model and the power-law model fitted to the concentration density values $\rho[A(\epsilon)]$, calculated as ppm/km^2 within square windows with various window sizes ϵ by least squares method. (A) Data plotted on a normal scale and (B) on a log–log scale.

Figure 2 Distribution of As values (ppm) in stream sediment samples with a sampling density of one mixed sample per 4 km^2. Black triangles represent Sn mineral deposits, and black lines represent faults. The green circle indicates a location for which (and the white square indicates a window within which) the concentration values of As were examined for singularity analysis (for more details, see the text).
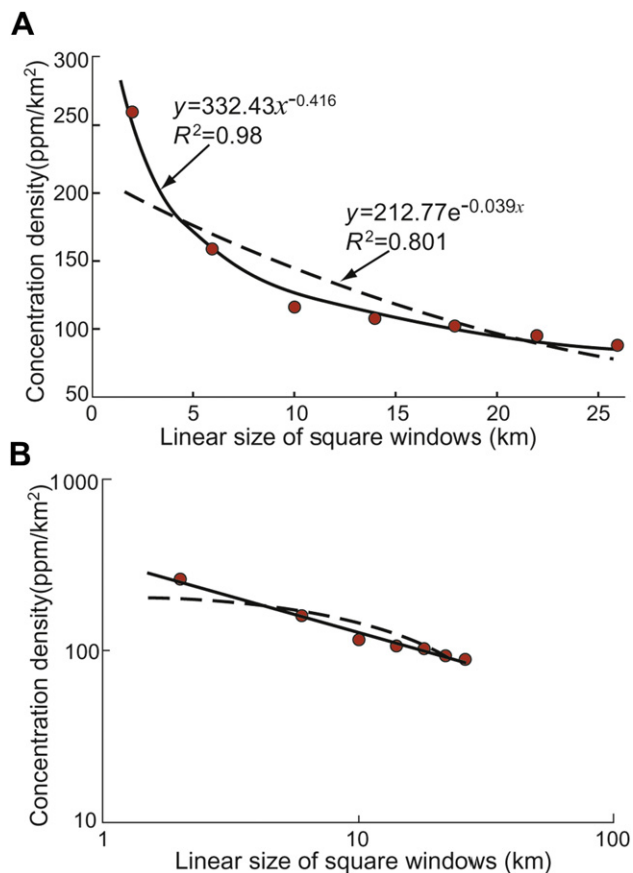
power-law model better fits the data, as confirmed by the larger correlation coefficient ($R^2 = 0.98$) for the power-law model than that for the exponential model ($R^2 = 0.801$). Comparing these two functions, we can see that the power-law function increases faster than the exponential function when the window size becomes very small. The power-law function does not converge, whereas the exponential function shows a continuous and smooth curve when A becomes very small. In other words, the power-law model characterizes the singularity of the distribution of concentration density, which tends to become anomalously high when the area becomes infinitely small. In contrast, the exponential model only shows a gentle and smooth increase at a rate of 2.8 ppm/km in this example.

3.2. Density-area power-law model and generalized self-similarity

It has been shown that power-laws might be a primary function for describing singular processes. Scale invariance is a unique property of power-law functions in which the type does not change when the scale changes. This type of property corresponds to self-similarity in geometry, and power-laws are the basic function of fractal geometry and multifractal fields. Therefore, fractal and multifractal modeling based on power-law functions provide powerful tools to characterize the scale invariance of geo-processes and geo-events. Multiple recent successes have been reported with the application of fractal and multifractals in the context of geocomplexity (Lovejoy et al., 2009). Although most fractal models are used to deal with isotropic scale invariance, several models have been investigated for modeling anisotropic scale invariance. A multifractal model has been proposed on the basis of extreme value distributions of 2D multifractal fields, stating that the concentration value (C) and the area enclosed by the cutoff concentration value ($A[>C]$) follow a power-law relation (Cheng et al., 1994):

$$A[> C] \propto C^{-\beta} \tag{8}$$

For a mineral district, Relation (8) may have several values of exponents. The area (A) involved in Relation (8) can be of any shape as long as the power-law relation in (8) holds true. Therefore, this concentration-area model (C-A model) becomes one of the original simple density-area models for characterizing anisotropic scale invariance. To illustrate the concentration-area model (8), we used a map with the same concentration values of Sn (ppm) in the stream sediment samples as the As values in Fig. 2. The results are shown in Fig. 4, where the colors represent the log-transformed values of Sn, and the superimposed contours are identified by means of C-A, as shown in Fig. 5. The plot in Fig. 5 shows that the values of C-A relationships can be fitted by power-law models with different exponents. Four classes of Sn values are grouped with three cutoff values identified using straight line fitting by a least squares method. Three cutoff values (2, 6 and 344 ppm) were estimated, and these values separate the Sn values into four groups labeled as (I), (II), (III) and (IV) in Fig. 5. Accordingly, three sets of contours were plotted to represent the three groups of (I), (II) and (III). The contours in Group IV are not shown here because this group represents background low values less than 2 ppm. It can be seen in Fig. 4 that the contours in Group I are of circular shape with a limited extension. Two large Sn deposits are located within this group. The contours in Group II show more complex shapes with two centers. Six mineral deposits are located in this group. Two mineral deposits are located in the region delineated by the contours in Group III. The concentration values and areas in these three ranges of values follow three different power-law relations with different exponents, as −3.1, −1.57 and −0.79, respectively. The slopes from I to III indicate the increase of singularities towards the centers of the geo-anomalies. Different slopes may also indicate some mixing of processes with various degrees of intensity of abnormalities. The contours shaping the spatial distributions of Sn in the area break up the values of the concentration-area relationships. These types of distinction in terms of self-similarity can be used to distinguish anomalous and background patterns.
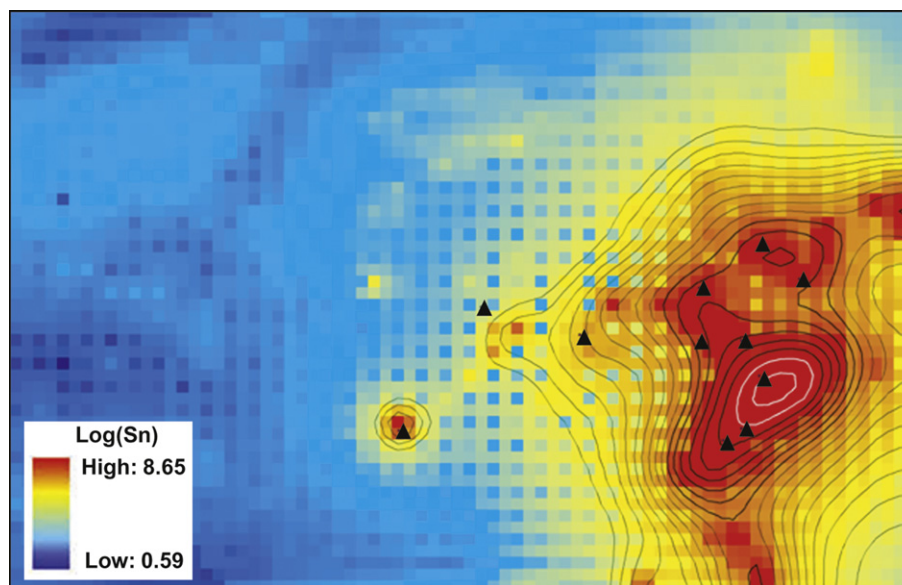

Figure 4 Distribution of log-transformed values (ppm) of Sn in stream sediment samples. Black triangles represent Sn mineral deposits. Smooth contour lines were created and classified using the breaks identified by means of the C-A plot shown in Fig. 5. White lines represent contours with values above 344 ppm, thick solid black lines represent values from 6 to 344 ppm, thinner black lines indicate values from 2 to 6 ppm, and contours with values below 2 ppm are not shown here.
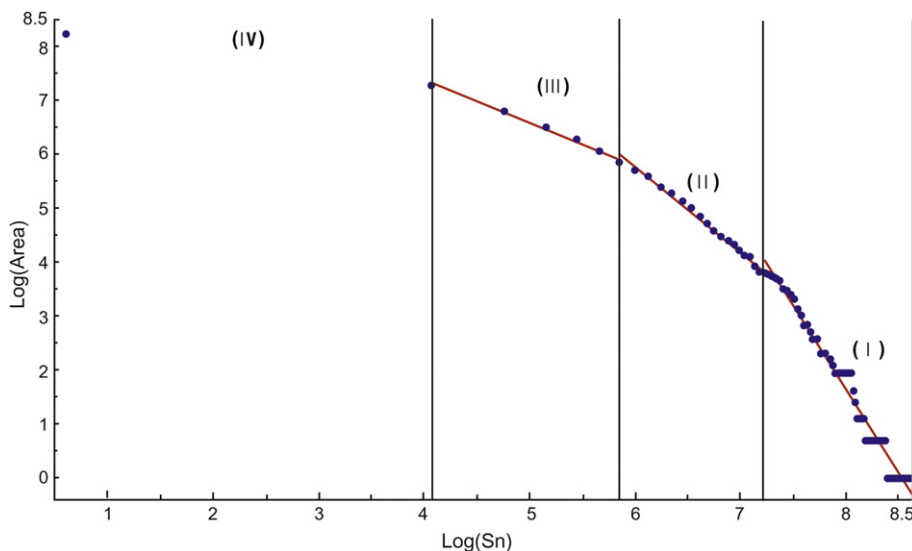
Figure 5 *C-A* (concentration-area) plot showing the cumulative area versus the tin concentration value; the base of logarithms is e. Three breaks at 2, 6 and 344 ppm separate the Sn values into four ranges; in three of these ranges, straight lines were fitted to the data by least squares method. The parameters for the three straight lines are the following: (I) slope −3.1, intercept 26.6 and standard error 0.036; (II) slope −1.57, intercept 15.2 and standard error 0.0027; and (III) slope −0.79, intercept 10.6 and standard error 0.0012. These breaks are used in Fig. 4 to classify the contours into four groups.

The idea of the *C-A* model was further extended to characterize the spectral energy density-area relation in frequency domains (Cheng et al., 1999):

$$A(\geq S) \propto S^{-2d/\beta} \tag{9}$$

where $S[\omega]$ stands for the spectral energy density at wave number vector ω, $A[\geq S]$ indicates the area in units of wave number with a threshold above S, the symbol $\propto$ stands for "proportional to", β is the anisotropic scaling exponent, and d is a parameter representing the degree of overall contraction (Cheng et al., 1999; Cheng, 2004). As the shape of A involved in these models (*C-A* and *S-A*) at different concentration levels (C) or spectral energy densities (S) can be any self-similarly shaped set (such as contours), these self-similar contours characterize the anisotropic scale invariance of the density distribution. Thus, the exponent of the power-law relation becomes an essential index that characterizes the generalized self-similarity, implying that a geo-field shows diversity in the spatial domain and self-similarity in a special domain such as a Fourier domain (Cheng, 2004). A more general formulation to represent the density-area relation can be expressed as follows:

$$< \rho[\Omega(A)]> = c\sqrt{A}^{-\Delta\alpha} \tag{10}$$

where ρ represents a type of density or quantity defined in a small area (or volume) in a mineral district $\Omega(A)$ with size A, c is a quantity independent of size A, and $\Delta\alpha = 2-\alpha$ is the singularity index (with α also known as the Hölder exponent; Mandelbrot, 1989). The singularity index $\Delta\alpha$ quantifies the degree of singularity. The symbol $<>$ stands for the expectation that power-law relations usually hold true in the statistical sense. Instead of a unique value of exponent $\Delta\alpha$, which would correspond to a single fractal, the values of c and α vary in the mineral district from place to place, corresponding to multifractals. Fractals are usually referred to as a property of geometry or a single statistical distribution, whereas multifractals are related to continuous fields or complex patterns defined on geometric sets that themselves can

be fractals. From this perspective, multifractal models have more applications in practice.

Although expressed as a density and area relationship, if treating the energy and mass and the time and space as exchangeable quantities, Model (10) can be adopted to represent the energy density−time relationship, which can be used to describe the singularity of temporal systems such as earthquakes and landslides.

3.3. Singularity and abnormality

One of the generic properties of the power-law relation is its singularity: when the scale becomes extremely small, some quantities derived from the power-law relation approach infinity; for example, the density ρ defined in Model (10) stays constant only if α has a value close to 2 or $\Delta\alpha = 0$; otherwise, if $\alpha < 2$ or $\Delta\alpha > 0$, the density approaches infinity, and, if $\alpha > 2$ or $\Delta\alpha < 0$, the density approaches zero. These properties of the power-law Model (10) imply that at a location where normal regional geological processes occurred without causing the enrichment or depletion of the concentration values of certain elements in rocks or other surface media, the concentration value density tends to be statistically constant, independent of the measuring area size. This is to say that the element concentration values in the region are linearly distributed. These types of regions correspond to geological background. In contrast, at other locations where mineralization occurred and caused element enrichment and depletion, the concentration value density is proportional to the measuring area size. This implies that the element concentration values in the region are nonlinearly distributed. These types of regions correspond to geo-anomalies. Therefore, the power-law model can be used in many cases to characterize geo-anomalies, and the value of $\Delta\alpha$ quantifies the degree of abnormality (Cheng, 2007c).

To demonstrate the concept and application of singularity analysis, we created a combined map from the concentration values of six elements (Sn, Cu, As, Pb, Zn and Cd) by means of principal component analysis with a correlation coefficient matrix

model. More information on the general use of principal component analysis (PCA) and some new extensions of PCA can be found in many references, such as Cheng et al. (2006). The first principal component reflects the combination of all six elements with evenly distributed positive loading. This element combination reflects the main elements association with Sn and Cu mineralization. The scores of the six elements on the first principal component were calculated and are shown in Fig. 6. The patterns in this figure generally show high values in the area of the Gejiu Formation and around the Gejiu batholith that are shown as transparent polygons. Therefore, the combined geochemical patterns represent the overlapped contributions of various geological features and processes. Square windows with various sizes ranging from 2 to 6 km up to 26 km were applied to calculate the singularity index α, and the results are shown in Fig. 7. More detailed information on the calculation of singularity can be found in Cheng (2007a). The results show that the areas around the mine sites correspond to strong Sn, As, Cu, Pb. Zn and Cd anomalies. Anomalies in the western part are generally weak. Clearly, the distribution of these elements cannot be directly used to delineate anomalies in the western part. The patterns of α values calculated from the combined map of these elements illustrate that the areas with α values < 2 are spatially coincident with the locations of most known Sn deposits. In addition, a number of anomalies are delineated in the western part of the study area. The results indicate that the areas with α values from 1.5 to 1.925 have the optimum spatial correlation between anomalies and known mineral deposits (Cheng, 2007a). This example demonstrates that mapping singularity from a geochemical map can provide useful information for geo-anomaly identification.

3.4. Diversity and generalized self-similarity

Diversity is a common property of nature. Mineralization also often shows diversity in terms of factors such as genesis types, commodities and ore bodies. Mineralization is usually associated with multiple factors such as the sources of ore materials,

interactions with country rocks and the formation environment, to name a few. These types of factors often lead to diverse mineralization and multiple types of mineral deposits. However, the generic property of the same type of mineralization often shows self-similarity. Diversity and self-similarity are two end members of a spectrum, but are these two properties totally distinct? In fact, diversity and self-similarity are just two end members of the spectrum containing generalized self-similarity in the middle. Generalized self-similarity represents a phenomenon in which the system shows diversity in one space but self-similarity in the other "genetic" space. For example, in the space domain, many species (including humans and plants) show diversity, as in different species, different colors, different shapes and so on, but these species have their own DNA series in their generic domains.

Diversity and self-similarity are fundamental properties of complex mineralization. If the power-law can be used as a genetic model to characterize mineralization as a singular process, the scale invariance, a unique property of the power-law function, guarantees some types of self-similarities of mineralization. Based on the power-law function, the quantities measured for two different scales can be associated by a scale transformation:

$$< \rho[\Omega(A_1)] > \; = (A_1/A_2)^{\alpha/2-1} < \rho[\Omega(A_2)] \rangle \qquad (11)$$

In order words, the value for one scale can be transformed from the value for another scale according to a scale transformation (Cheng, 1999). Typical examples of power-law relationships include geophysical potential fields such as magnetic and gravity fields, which possess self-similarity with respect to the distance (or height) between the sensor and the source of the geological body. For example, the magnetic and gravity fields at any height above the ground can be calculated from corresponding fields measured on or near the ground by an upward continuation transformation (Cheng and Xu, 1998). Another example involves the geochemical halos associated with and around ore bodies. As the distance from an ore body increases, the intensity of the halo statistically decreases. In addition to intensity changes, the assemblages of minerals or elements may also gradually change.
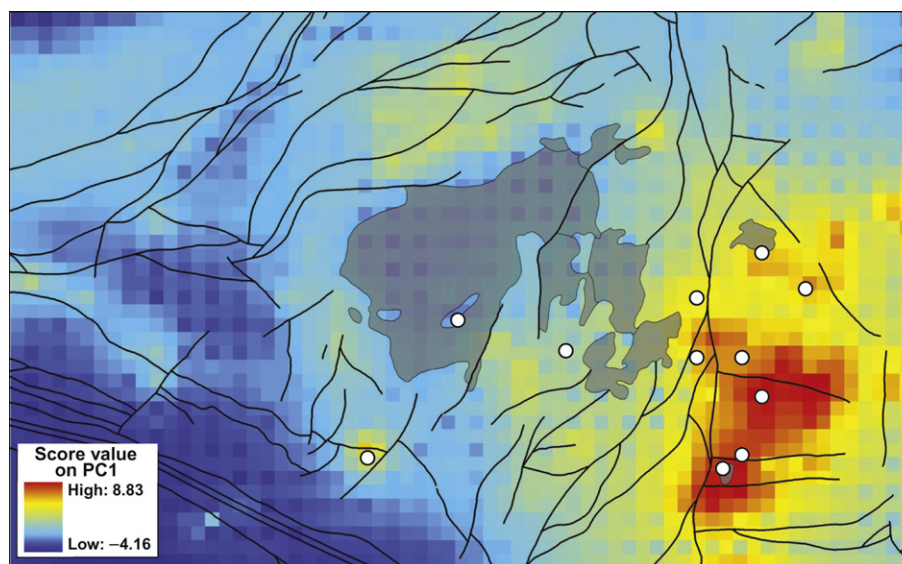

Figure 6 Scoring map of the first principle component showing the spatial distribution of multiple elements of Sn, Cu, As, Pb, Zn and Cd. Transparent polygons located in the middle of the figure indicate intrusive bodies, solid black lines represent faults, and white dots represent Sn mineral deposits.
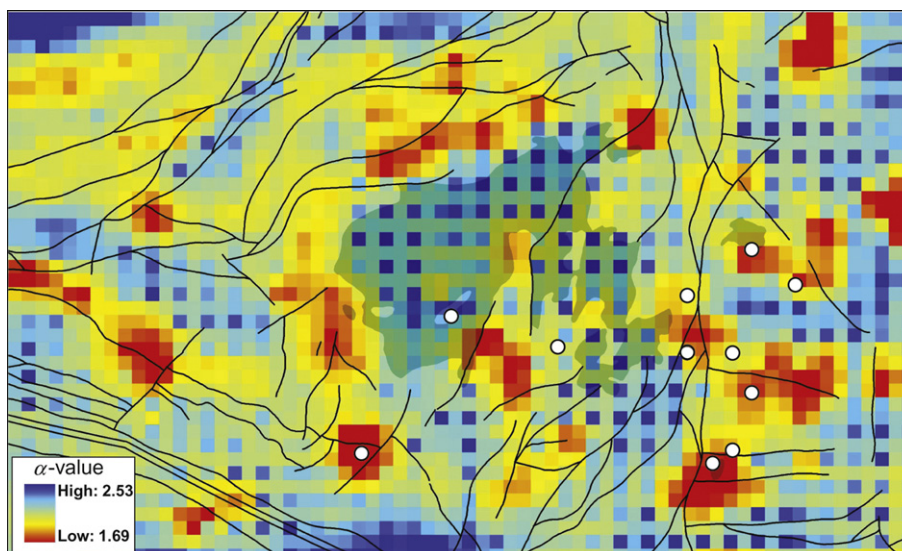
Figure 7   Singularity obtained from the anomalies in Fig. 6, with a positive value of 5 added so that the map has positive values. Singularity was calculated with square windows sized within 26 km.

This is the principle behind identifying primary geochemistry halos to assist in allocating ore bodies. The zoning of halos identified in terms of both intensity and element associations is useful for reducing target areas to find ore bodies. In field observations, geologists seek self-similarity between structures at different scales, and these scale relationships can be used to infer large-scale structures by examining the small-scale structures observed on specimens and even under microscopes.

The patterns represented at two different scales look similar if they are associated with scale transformation or possess a scale invariance property. Recent studies have demonstrated that self-similarity can be characterized by more complex anisotropic and nonlinear scale transformations; for example, self-affine transformation can be applied, corresponding to self-affinity (stratification), and even more complex transformations such as GSI (generalized scale invariance transformation; Schertzer and Lovejoy, 1987) and irregular contour-based methods (Cheng, 2007d) can be applied. These types of properties show self-similarity characterized as a power-law in a special domain (not the space domain), but diversity in the space domain can be named generalized self-similarity (Cheng, 2007b). The identification of generalized self-similarity is useful for the separation of anomalies according to the distinctive generalized self-similarity observed in other domains such as the Fourier Domain and Eigen Domain. Several power-law models, including S-A (Cheng et al., 1999) and N-λ (Cheng, 2005), have been developed in these domains to separate anomalies for mineral resource assessments.

To apply the power spectral energy density-area model (S-A) to decomposing mixing patterns, the map in Fig. 6 was converted into a frequency domain by means of fast Fourier transformation. Two components (the power energy density and phases) were obtained by Fourier transformation. The former is shown in Fig. 8A. On the power spectral energy plane, various thresholds of power spectral energy density were set, and the areas enclosed with the thresholds were plotted on a log-log plot (Fig. 8B). Two straight lines were fitted to the data by least squares method. These two lines separate the values into two ranges with the cutoff value of $S = 1919$, where the distinct scaling properties of the S-A relation are maintained in each. The slopes of these two straight lines are significantly

different, indicating that the power energy density values show significantly different self-similarity attributes. The cutoff value of $S = 1919$ was used to define two filters: one consists of wave numbers with $S \leq 1919$ (as the anomaly filter), and one uses $S > 1919$ (as the background filter). The shapes of the two filters are irregular and maintain the anisotropic properties and spatial structure of the geochemical pattern. Within these two filters, S and A follow two distinct power-law relations, each with its own exponent, implying that the signals in these ranges are self-similar.

Applying the two filters with ranges of S defined as anomaly and background in Fig. 8B to the fast Fourier-transformed functions and then converting them back to the spatial domain using inverse Fourier transformation, two decomposed maps were created and are shown in Fig. 9A and B. Fig. 9A represents the background component of the geochemical landscape of the multiple elements, which generally highlights two sub-regions separated in the middle of the Gejiu batholith; the eastern region shows high background, and the western region shows low background. Fig. 9B shows the anomalies located not only in the eastern region (coinciding with known mineral deposits), but also in the western region. The anomalous areas shown in Fig. 9B are either spatially in good agreement with the locations of known mineral deposits or are present along faults or around fault intersections. The decomposed anomalous and background patterns shown in Fig. 9A and B are explicitly different, each corresponding to a distinct self-similarity in the Fourier domain characterized by a different power-law model. This example shows that the generalized self-similarity principle can be used to develop fractal filtering techniques for decomposing mixing patterns, which is an essential task for mineral exploration.

4. Spectrum and multifractality of singular mineralization

It has been demonstrated that the power-law is a fundamental model capable of describing the density-area relationships involved in a geochemical landscape affected by mineralization. The exponent of such power-laws is a key parameter that is often related to the
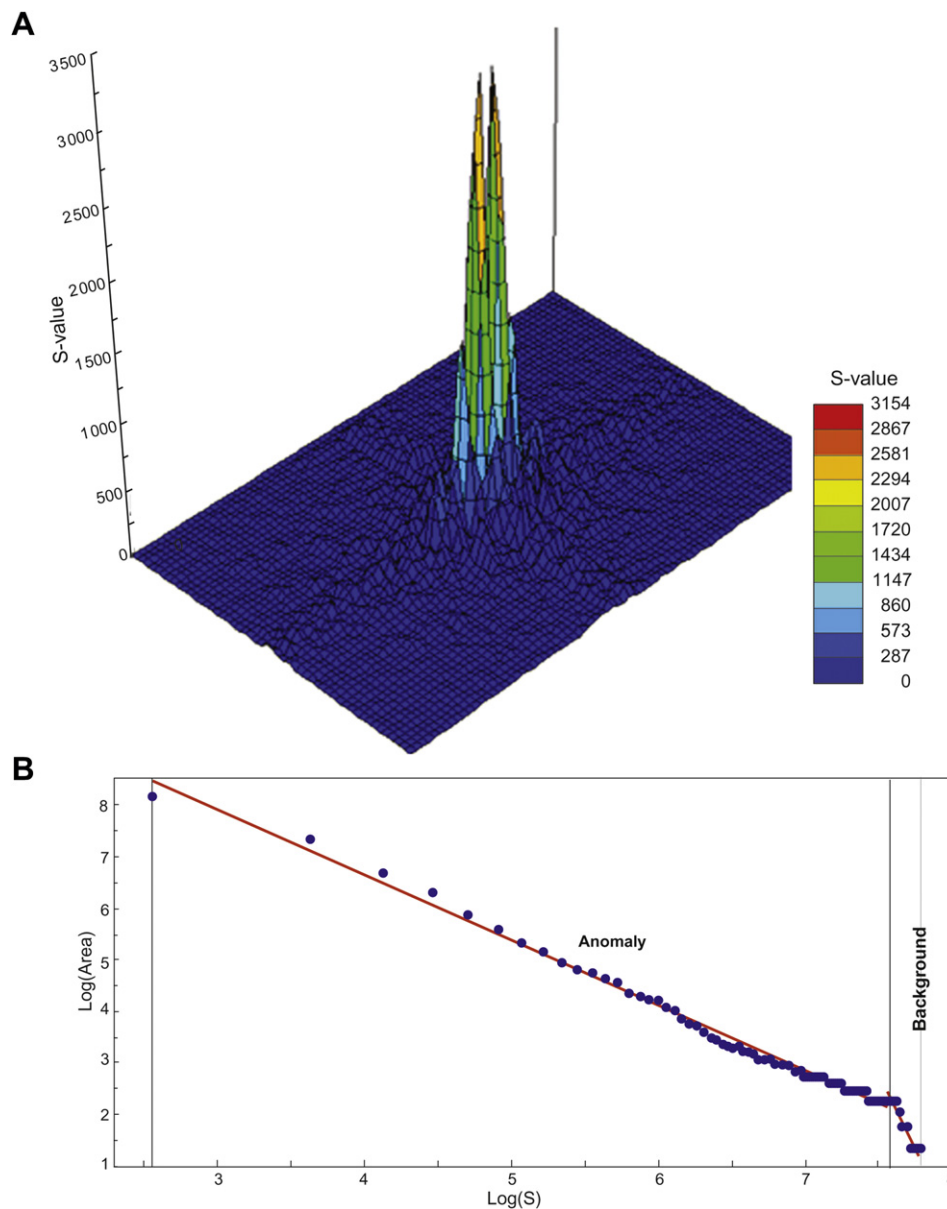
Figure 8 (A) Spectrum energy density map (S) calculated using fast Fourier transformation. Center of the map indicates the origin of the wave number. (B) S-A plot showing the relationship between power energy density S and area A. The meaning of S and A are explained in the text. The solid lines are fitted by least squares method. The break point separating the two straight lines is estimated as $S = 1919$.

dimension of the sets or the fractal density (Cheng, 2007b). Dimensions are important quantities of nature, including geometries and the fields defined on geometry. Objects can be classified into groups according to their dimensions as points, lines, polygons and volumes, and, in addition, objects can be classified based on non-integer dimensions. Objects with the same dimensions depict similar properties, whereas those with different dimensions often show different properties. More generally, measures or fields defined for objects with different dimensions are also distinguishable. This is the main principle for the utilization of the concepts and methods of singularity and generalized self-similarity in anomaly identification and decomposition. So far, we have introduced only the processes applied to maps created for either single elements or group elements. In mineral exploration, however, multiple factors and maps are often needed to comprehensively delineate prospective areas for mineral prospecting. Geo-anomalies often correspond

to other aspects of anomalies such as geochemical and geophysical anomalies due to chemical and physical property differences between the geo-anomalies and background. The idea and model of singularity can be extended to deal with multiple geo-anomalies. For example, the posterior probability of a unit area containing mineral deposits was used to represent multiple geo-anomalies from the point of view of multiplicative cascade processes (Cheng, 2008). Multiplicative cascade processes are nonlinear processes common in geosciences that can create end products with multi-scale singularities following multifractal distribution (Agterberg, 2005). Some mineralization processes possess the property of multiplicative cascade processes, each causing the redistribution of elements in the crust, with some areas being depleted and others enriched (de Wijs, 1951; Schertzer et al., 1997). The amount of metal in a given area of the mineralization domain may show a power-law distribution related to the size of the area. Singularity is a natural property
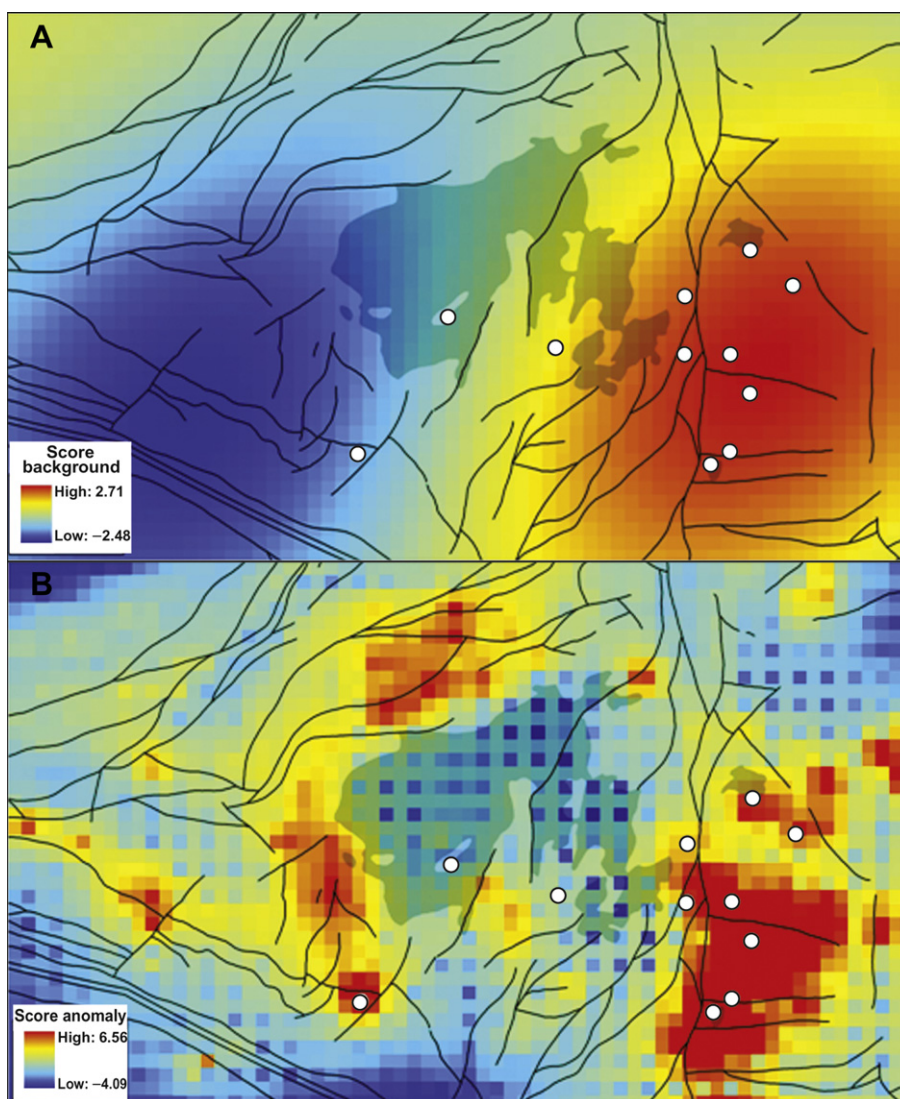
Figure 9   Decomposed geochemical maps obtained by using a fractal filtering technique. (A) Background component obtained by the fractal filter defined as $S > 1919$; (B) anomalies obtained by the fractal filter defined as $S \leq 1919$, from Fig. 8B.

of mineralization, which involves the enrichment and depletion of ore and associated elements in the Earth's crust as well as in other relevant secondary media such as tills, soils, lake and stream sediments, humus and the vegetation surrounding mineral deposits. Mapping such singularities is an effective way to delineate areas favorable for the occurrence of mineral deposits and to estimate the likelihood of the presence of mineral resources in a given area. If we define the chance of a unit area containing mineral deposits as a type of density O(D), where D indicates deposits and O indicates the standard for the Odds of D, then the variability of such chance may also show singularity. Chance O(D) is related to probability P(D) by O = P/(1−P) or P = O/(1 + O). Therefore, the probability of a unit area containing mineral deposits can also be used to characterize the variability in the chance of having mineral deposits. The probability might be easy to understand and interpret for geologists. If a unit area is randomly selected from a district without considering the property of the unit area, then the probability of such a unit area containing deposits is called the prior probability. The probabilities of unit areas selected from certain areas with some conditions are called posterior probabilities. One can map the posterior

probabilities by combining multiple maps related to the location of mineral deposits with various integration models such as weights of evidence, logistic regression, fuzzy logic or neural networks (Bonham-Carter, 1994). This is an essential task in the quantitative prediction of mineral deposits and in mineral resource quantitative assessment. Such a predictive map can assist the spatial decision-making in mineral exploration and mineral resource planning. The formulation of the such processes can be expressed as P(D) = P (D|AB…), where the posterior probability is a function of multiple maps (A and B, etc.) that are prepared to predict mineral deposits. Adding each of these maps (evidence layers) will reduce the study into small areas, each with unique conditions of evidence, and the posterior probability of these small areas can be updated. These processes eventually lead to a final posterior probability map, on which some small areas delineated by combining multiple patterns positively associated with the location of mineral deposits will have very high posterior probabilities (much higher than the prior probability). In contrast, most areas delineated with negatively associated patterns will show very low posterior probabilities (much lower than the prior probability). Based on the posterior probability map

created by combining multiple geo-evidence layers, various power-law models can be applied to characterize the singularity of the posterior probability map.

To demonstrate the application of data integration processes for creating posterior probability maps, we combine the following four layers of patterns to map the posterior probability of Sn mineral deposits in the Gejiu district. These four layers (Cheng et al., 2009) are: (1) the carbonate Gejiu Formation labeled as the yellow patterns in Fig. 1; (2) the 6-km buffer zones around the intersections of three groups of faults (faults are shown as black lines in Fig. 1); (3) local geochemical anomalies extracted by principal component analysis applied to local singularity indices calculated for the elements Sn, As, Zn, Pb, Cu and Cd (results not shown); and (4) regional geochemical anomalies (Fig. 9B) extracted by the S-A fractal filter method. More detailed information on the definition of the four binary layers can be found in Cheng et al. (2009). Each of these four information layers divides the study area into two subclasses representing favorable and unfavorable regions for the prediction of mineral deposits. The final posterior probability map created by combining these four layers using the weights of evidence method is shown in Fig. 10A.

More evidence layers can be added to generate more detailed posterior probability maps. These types of maps show singularities in some places that have high posterior probabilities within very small areas, which can be characterized by density (posterior probability)–area fractal relations. The most interesting areas are those with high posterior probabilities, but no known discovered mineral deposits. Areas with high posterior probabilities can be considered as multiple geo-anomalies that must show strong singularities. For example, high posterior probabilities are plotted against the area of each combination of evidential layers in Fig. 10B. The horizontal axes represent the log-transformation of the probability of the area of classes with posterior probabilities above a threshold; the vertical axes represent the log-transformation of the posterior probability. The result shows a power-law relation between the cumulative area and the cutoff value of posterior probability. From the power-law relationship, a singularity index as $\alpha = 0.93 < 2$ or $\Delta\alpha = 2-0.93 = 1.07$ was estimated, and this value implies a strong enrichment of the posterior probability at the peaks when the size of area G decreases.

5. Nonlinear methods for information extraction and information integration required for the quantitative assessment of mineral resources

Three fundamental properties of mineralization (geo-anomaly, mineral diversity and mineral deposit spectrum) have been considered for a so-called "three-component" mineral resource assessment method (Zhao, 2002). From the point of view of multifractal-based nonlinear theory, these three aspects also
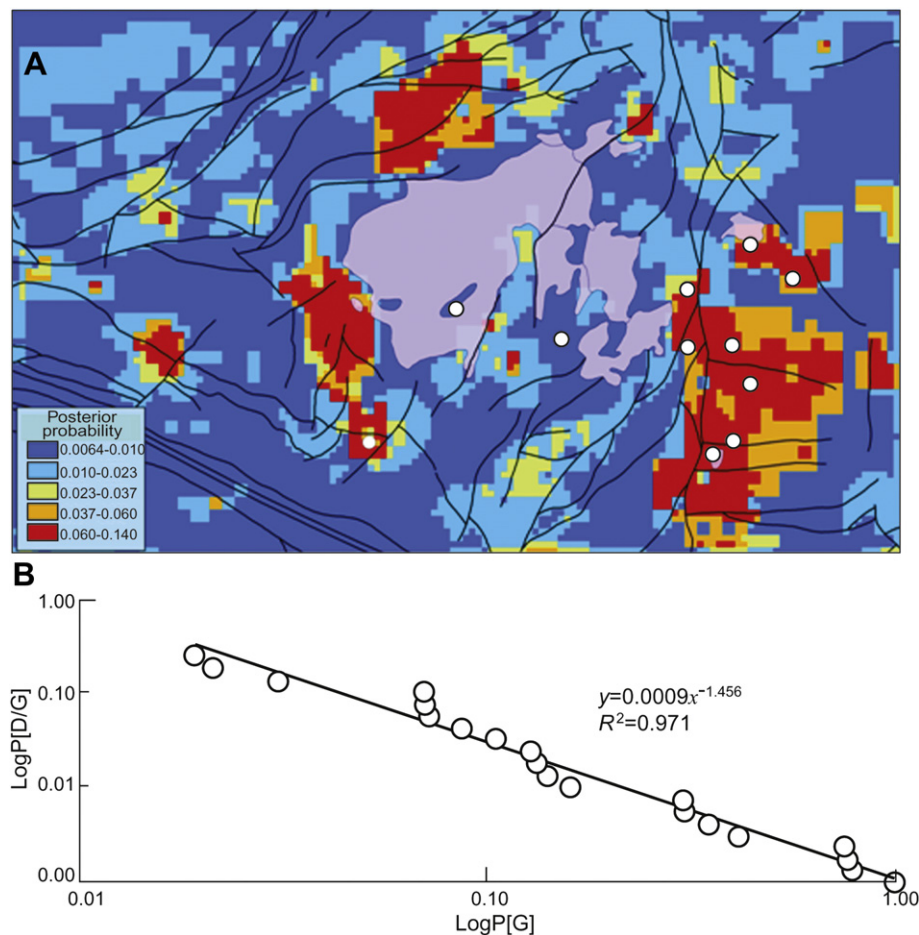

Figure 10 (A) Posterior probability map created by means of a weights of evidence method applied to the four evidential layers. (B) Plot showing the relationship between the posterior probability and the area above the cutoff value of posterior probability.
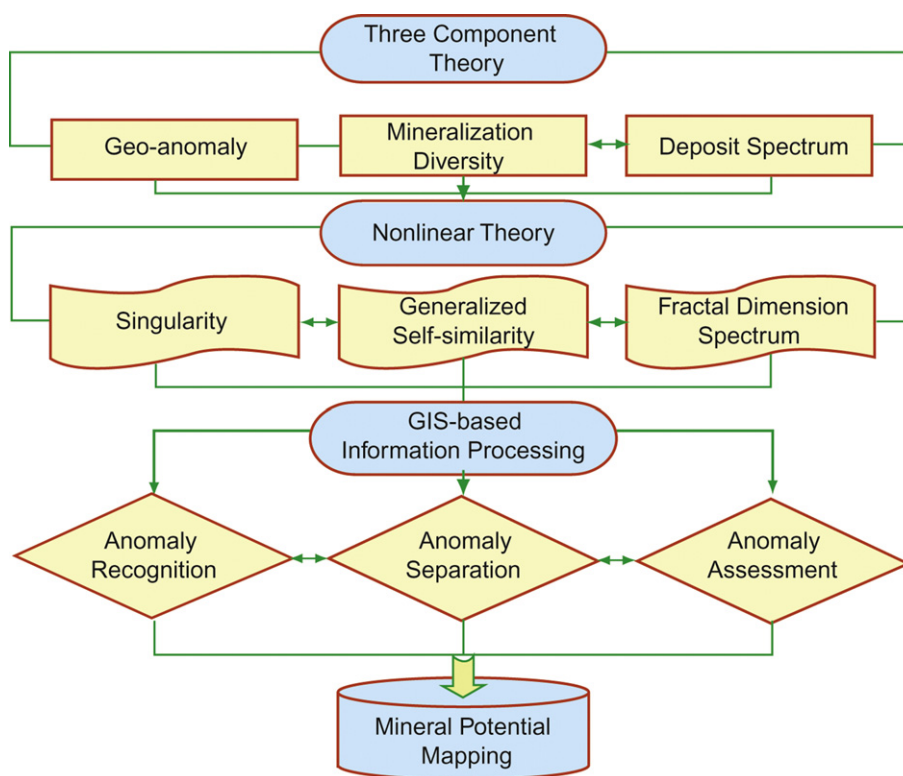
Figure 11   Flowchart showing the concepts of geo-anomaly and singularity and the methods for information processing and mineral resource prediction.

represent the fundamental properties of nonlinear processes, which can be characterized using multifractal modeling of, for example, the singularity, generalized self-similarity and fractal spectrum. These three components of mineralization must be considered for mineral resource assessments characterizing the fundamental properties of mineralization, whereas singularity theory and related multifractal models provide quantitative solutions to quantify these properties of mineralization and are essential for mineral deposit predictions and mineral resource quantitative assessments. In addition, the nonlinear singularity theory emphasizes the dynamics of mineralization and naturally associates the dynamics and products of mineralization. Furthermore, these nonlinear models can be applied to quantitatively processing geo-information to identify anomalies, decompose mixed anomalies and evaluate the association between anomalies and mineral deposits. The associations between the "three components" and "3S" (singularity, generalized self-similarity, multifractal spectrum) for mineral resource quantitative assessments and for mineral deposit predictions can be illustrated in the flowchart (Fig. 11). The singularity concepts and its related mathematical models have been developed and applied to mineral potential mapping and have especially proved to be effective for the integrated prediction of mineral resources in covered areas or of mineral deposits buried at significant depths. Singularity mapping provides a powerful tool to extract weak anomalies either caused by buried sources or affected by covers. Generalized self-similarity methods such as the *S-A* method can be used to decompose complex anomalies with various backgrounds, and data integration methods and the principles of multiplicative cascade processes (such as the weights of evidence method) can be used to fuse diverse geo-evidential layers with unbalanced or incomplete informatics between model areas and predicting areas

or between outcropped areas and covered areas. These techniques and models have been implemented in GeoDAS, a specialized GIS that has been widely applied in the mineral industry, including in various national projects on mineral potential prediction and mineral resource assessments in China.

6. Conclusions

Geo-anomalies, a fundamental characteristic of mineralization processes, can be quantitatively characterized by means of singularity. Nonlinear models and methods related to singularity can provide powerful tools for the quantification of the characteristics of geo-anomalies and for the identification of geo-anomalies to delineate target areas for mineral exploration. The local singularity analysis method can be effectively employed to map geo-anomalies to delineate favorable areas for single geo-variables of undiscovered mineral deposits. The new singularity model in conjunction with data (map) integration processes provides a tool to map posterior probabilities by combining multiple geo-variables (evidence). Data integration treated as a generalized form of multiplicative cascade processes can generate posterior probabilities with singularity, which can be characterized by a density-area power-law model. A generalized self-similarity principle can be applied to separate mixing anomalies to represent different background geo-processes and metallogenic processes. Fractal spectra represented by various power-law models such as the concentration-area model, number-size model, grade-tonnage model and posterior probability model, can be utilized to characterize geo-anomalies and for the purposes of mineral deposit prediction. Although introducing singularity and its related nonlinear theories and methods into the study of geo-anomaly may not completely cover the scope of geo-anomaly theory

in mineral resource assessment, the integration of geo-anomalies and singularity demonstrates that modern nonlinear theory may provide new directions for further geo-anomaly studies.

Acknowledgements

References

Agterberg, F.P., 1995. Multifractal modeling of the sizes and grades of giant and supergiant deposits. International Geology Review 37, 1−8.

Agterberg, F.P., 2005. Application of a three-parameter version of the model of de Wijs in regional geochemistry. In: Cheng, Q.M., Bonham-Carter, G.F. (Eds.), GIS and Spatial Analysis. China University of Geosciences Printing House, Wuhan, pp. 291−296.

Bonham-Carter, G.F., 1994. Geographic Information Systems for Geoscientists: Modeling with GIS. Pergamon, Oxford, p. 398.

Cheng, Q.M., 1999. Multifractality and spatial statistics. Computers & Geosciences 25 (10), 949−961.

Cheng, Q.M., 2001. The decomposition of geochemical map patterns on the basis of their scaling properties in order to separate anomalies from background. Bulletin of the International Statistical Institute 59 (2), 481−484.

Cheng, Q.M., 2004. A new model for quantifying anisotropic scale invariance and decomposing of complex patterns. Mathematical Geology 36 (3), 345−360.

Cheng, Q.M., 2005. Multifractal distribution of eigenvalues and eigenvectors from 2D multiplicative cascade multifractal fields. Mathematical Geology 37, 915−927.

Cheng, Q.M., 2007a. Mapping singularities with stream sediment geochemical data for prediction of undiscovered mineral deposits in Gejiu, Yunnan Providence, China. Ore Geology Reviews 32 (1−2), 314−324.

Cheng, Q.M., 2007b. Multifractal imaging filtering and decomposition methods in space, Fourier frequency, and Eigen domains. Nonlinear Processes in Geophysics 14 (3), 293−303.

Cheng, Q.M., 2007c. Singular mineralization processes and mineral resources quantitative prediction: new theories and methods. Earth Science Frontiers 14 (5), 42−53.

Cheng, Q.M., 2007d. GIS based fractal/multifractal anomaly analysis for modeling and prediction of mineralization and mineral deposits. In: Harris, J., Wright, D. (Eds.), GIS for Geosciences. Geological Association of Canada, pp. 285−296.

Cheng, Q.M., 2008. Non-linear theory and power-law models for information integration and mineral resources quantitative assessments. Mathematical Geosciences 40, 503−532.

Cheng, Q.M., Agterberg, F.P., 2009. Singularity analysis of ore-mineral and toxic trace elements in stream sediments. Computers & Geosciences 35, 234−244.

Cheng, Q.M., Agterberg, F.P., Ballantyne, S.B., 1994. The separation of geochemical anomalies from background by fractal methods. Journal of Geochemical Exploration 51 (2), 109−130.

Cheng, Q.M., Jing, L., Panahi, A., 2006. Principal component analysis with optimum order sample correlation coefficient for image enhancement. International Journal of Remote Sensing 27 (16), 3387−3401.

Cheng, Q.M., Xu, Y., 1998. Geophysical data processing and interpreting and for mineral potential mapping in GIS environment. In: Buccianti, A., Nardi, G., Potenza, R. (Eds.), Proceedings of the Fourth Annual Conference of the International Association for Mathematical Geology, 2. De Frede Editore, Napoli, Italy, pp. 394−399.

Cheng, Q.M., Xu, Y., Grunsky, E., 1999. Integrated spatial and spectral analysis for geochemical anomaly separation. In: Lippard, S.J., Naess, A., Sinding-Larsen, R. (Eds.), Proceedings of the Fifth Annual Conference of the International Association for Mathematical Geology, 1, pp. 87−92. Trondheim, Norway.

Cheng, Q.M., Zhao, P.D., Zhang, S.Y., Xia, Q.L., Chen, Z.J., Chen, J.G., Xu, D.Y., Wang, W.L., 2009. Application of singularity theory in prediction of tin and copper mineral deposits in Gejiu district, Yunnan, China: information integration and delineation of mineral exploration targets. Earth Science—Journal of China University of Geosciences 34 (2), 243−252.

de Wijs, H.J., 1951. Statistics of ore distribution, part I. Geologie & Mijnbouw 13, 365−375.

Lovejoy, S., Agterberg, F.P., Carsteanu, A., Cheng, Q.M., Davidsen, J., Gaonac'h, H., Gupta, V., L'Heureux, I., Liu, W., Morris, S.W., Sharma, S., Shcherbakov, R., Tarquis, A., Turcotte, D., Uritsky, V., 2009. Nonlinear geophysics: why we need it. EOS. Transactions, American Geophysical Union 12 (1), 455−456.

Mandelbrot, B.B., 1989. Multifractal measures, especially for the geophysicist. Pure & Applied Geophysics 131, 5−42.

Schertzer, D., Lovejoy, S., 1987. Physical modeling and analysis of rain and clouds by anisotropic scaling of multiplicative processes. Journal of Geophysical Research 92, 9693−9714.

Schertzer, D., Lovejoy, S., Schmitt, F., Chigirinskaya, Y., Marsan, D., 1997. Multifractal cascade dynamics and turbulent intermittency. Fractals 5, 427−471.

Turcotte, D.L., 1997. Fractals and Chaos in Geology and Geophysics, second ed. Cambridge University Press, England.

Xie, X., Mu, X., Ren, T., 1997. Geochemical mapping in China. Journal of Geochemical Exploration 60 (1), 99−113.

Zhao, P.D., 2002. "Three Component" quantitative resource prediction and assessment: theory and practice of digital mineral prospecting. Earth Science-Journal of China University of Geosciences 27 (5), 139−148.

Zhao, P.D., 2007. Quantitative mineral prediction and deep mineral exploration. Earth Science Frontiers 14 (5), 1−10.

Zhao, P.D., Chen, J., Zhang, S., 2005. Mineral deposit: geological anomalies wit high economic value. In: Cheng, Q., Bonham-Carter, G.F. (Eds.), Proceedings of IAMG'05, pp. 1022−1027.

Zhao, P.D., Chen, Y., 2001. Geoanomaly: the extreme value in geology and its application in quantitative assessment of mineral resources. Bulletin of the International Statistical Institute 59 (2), 477−480.

Zhao, P.D., Chi, S., 1991. Discussion of geo-anomaly. Earth Sciences 16 (3), 241−248.

Zhuang, Y., Wang, R., Yang, S., Yi, J., 1996. Geology of Gejiu Tin-copper Polymetallic Deposit. Earthquake Publishing House, Beijing, 189 pp.